Influence of the magnetic field on isotropic wetting behavior of a nematic liquid crystal

Erfan Kadivar[1,*]
[1]*Department of Physics, Faculty of Sciences, Persian Gulf University, 75168 Bushehr, Iran*
(Received 1 January 2008; published 10 September 2008)

I present a theoretical investigation of the temperature and magnetic field dependence of isotropic (paranematic) wetting layers close to an aligning substrate within a semi-infinite nematic liquid crystal with positive magnetic anisotropy under condition of weak homeotropic anchoring. Using the Landau–de Gennes model supplement by Nobili-Durand surface free energy, the existence and stability of paranematic wetting layers close to the substrate and below the nematic-isotropic temperature are discussed. Numerical results are presented showing the phase diagram for the isotropic (paranematic), nematic, and wetting layer states. In the present work, the dependence of the transition kind to the magnetic field is discussed.

DOI: 10.1103/PhysRevE.78.031706 PACS number(s): 61.30.Hn, 61.30.Gd

I. INTRODUCTION

The study of surface-induced ordering in liquid crystals is of special importance, not only for technological applications but also from a fundamental scientific point of view (for reviews see [1,2]). The phenomenon of the orientation of bulk liquid crystal director $\vec{n}$ (the average direction of the long molecular axis of the rodlike molecules) at an interface is called anchoring. Common anchoring states observed in experimental systems are homeotropic anchoring ($\vec{n}$ being parallel to the interface normal $\vec{z}$), planar unidirectional anchoring ($\vec{n} \perp \vec{z}$ in connection with a preferred in-plane direction of $\vec{n}$), and planar degenerate anchoring ($\vec{n} \perp \vec{z}$ with all in-plane directions being equivalent). The calculation of wetting behavior as a function of anchoring strength for homeotropic anchoring in planar geometry [3] and curvature geometry was studied in detail [4,5].

Wetting phenomena under an external bulk field were first studied for magnetism [6,7]. The possibility of inducing the prewetting transition by an external magnetic (or electric) field in nematic liquid crystals was first studied by Poniewierski and Sluckin [8] who used the Maier-Saupe mean field model. As is well known, the Maier-Saupe model fails for quantitative predictions [9–11]. In view of experimental results [12] on the electric field induced bulk isotropic-nematic transition, which are in good quantitative agreement with the predictions of the Landau–de Gennes model [12,13], it seems natural to use this latter model in the description of the prewetting transition under an external bulk field.

Landau–de Gennes models [3,14–17] and microscopic theories [18–24] predict a large variety of different pretransitional wetting behaviors as the anchoring at an interface is changed from homeotropic to planar.

II. LANDAU-GINZBURG–DE GENNES THEORY

In this paper by using the Landau–de Gennes theory, wetting phenomena will be investigated when an external magnetic field **H** is applied along the z axis. This is very important because many of the applications of liquid crystals are related to their ability to respond strongly to such external stimuli. Suppose that a static magnetic field H is applied to a nematic liquid crystal in the semi-infinite space ($z>0$) bounded on one side by a planar interface at $z=0$. To study wetting phenomena one can start with the Landau–de Gennes theory. This theory is based on traceless second-rank tensor **M**. It is either defined macroscopically through the traceless part of any second-rank material tensor such as the dielectric tensor ε or by starting from a microscopic definition as follows:

$$M_{ij} = \left\langle \hat{\nu}_i \hat{\nu}_j - \frac{1}{3}\delta_{ij} \right\rangle, \tag{1}$$

where the unit vector $\hat{\nu}$ indicates the directions of single molecules and $\langle \ldots \rangle$ means the average over all molecules in a sufficiently large volume. The Landau-Ginzburg–de Gennes free energy density in the presence of a magnetic field is obtained [25,26] as follows:

$$f(\mathbf{M}) = \frac{1}{2}a_0(T-T^*)M_{ij}M_{ij} - \frac{1}{3}bM_{ij}M_{jk}M_{ki} + \frac{1}{4}c(M_{ij}M_{ij})^2 + \frac{1}{2}L_1(M_{ij,k})^2 - \frac{1}{2}\Delta\chi H_i H_j M_{ij}, \tag{2}$$

where the summation over repeated indices is implied and the symbol, k means spatial derivative with respect to the spatial coordinate x_k. The first three terms on the right-hand side describe the transition from the isotropic to the nematic phase (in the absence of an external field) when the temperature T is lowered; a_0 and c are positive constants and T^* denotes the supercooling temperature of the isotropic phase. In the fourth term, one adopts, for simplicity, the one-constant approximation of the elastic energy which penalizes any nonuniform orientational order. The last term comes from the contribution of the magnetic field. When $\Delta\chi$ is positive, the molecules then tend to align parallel to the magnetic field. Thus, when a magnetic field is added to a uniaxial phase with positive $\Delta\chi$, the director will be parallel to the magnetic field and the effect is a slight increase of the uniaxial ordering. The experimental work of Boamfa *et al.* on wetting phenomena is based on this fact [27]. In the case

*erfan.kadivar@pgu.ac.ir

that $\Delta\chi$ is negative, the molecules tend to align perpendicular to the magnetic field direction. Thus the field direction introduces a second axis and the phase becomes biaxial [25]. My attention is restricted to the uniaxial nematic phase with positive $\Delta\chi$. Thus the uniaxial phase is stable when a magnetic field is applied.

The simplest quadratic surface free energy for nondegenerate ordering was proposed by Nobili-Durand [28] as follows:

$$F_s = \frac{W}{2}\int d^2x(M_{ij} - M_{ij}^{(0)})^2, \tag{3}$$

where $\mathbf{M}^{(0)}$ is the order parameter preferred by the surface and the surface-coupling strength W is positive.

The number of parameters is reduced considerably by using a rescaled order parameter $Q_{ij}=M_{ij}/g$ $[g=2\sqrt{6}b/9c]$ and temperature $\tau=a_0(T-T^*)/cg^2$. Furthermore, all lengths and the free energy are given, respectively, in units of $\xi=\sqrt{L_1/cg^2}$ and $\Delta f\xi^3=cg^4\xi^3$, where $2\sqrt{2}\xi$ denotes the nematic coherence length at the nematic-isotropic phase transition. Introducing the dimensionless surface-coupling parameter $\gamma=W\xi/L_1$, the reduced total free energy reads as follows:

$$F = \frac{1}{2}\int d^3x\left(\tau Q_{ij}Q_{ij} - \frac{\sqrt{6}}{2}Q_{ij}Q_{jk}Q_{kl} + \frac{1}{2}(Q_{ij}Q_{ij})^2 + (Q_{ij,k})^2 - \frac{\Delta\chi}{cg^3}H_iH_jQ_{ij}\right) + \frac{\gamma}{2}\int d^2x(Q_{ij} - Q_{ij}^{(0)})^2. \tag{4}$$

A uniaxial order parameter

$$Q_{ij} = S\left(n_in_j - \frac{1}{3}\delta_{ij}\right), \tag{5}$$

where $\mathbf{n}$ is the nematic director, S is the Maier-Saupe scalar order parameter, and δ_{ij} is the Kronecker symbol.

In the homeotropic anchoring configuration, the director field $\mathbf{n}=\mathbf{e}_z$ is oriented along the surface normal. Since parallel to the interface no direction of the molecules is preferred, I chose a uniaxial preferred order parameter

$$Q_{ij}^{(0)} = S_0\left(e_{zi}e_{zj} - \frac{1}{3}\delta_{ij}\right), \tag{6}$$

in the Nobili-Durand surface free energy. Assuming furthermore that the liquid-crystal ordering is uniform in x and y directions, the free energy (4) is converted into a free energy per unit area for the Maier-Saupe order parameter $S(z)$.

$$F_A[S(z)] = \int_0^\infty \left[f_b + \left(\frac{dS}{dz}\right)^2\right]dz + \gamma[S(0) - S_0]^2, \tag{7}$$

with the bulk free energy density

$$f_b = \tau S^2 - \frac{1}{\sqrt{6}}S^3 + \frac{1}{3}S^4 - hS, \tag{8}$$

where $h=\frac{H^2\Delta\chi}{cg^3}$ is the reduced magnetic field.

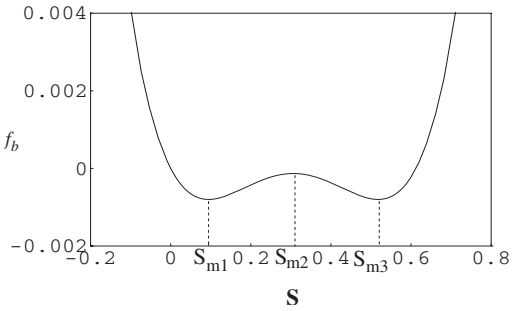

FIG. 1. Schematic drawing of the free energy versus order parameter S according to Eq. (8) for $h=0.02$ and $\tau_{NI}\approx 0.158$.

Bulk nematic-paranematic phase transition temperature in a nonzero magnetic field

In the zero field, by minimizing the first three terms on the right-hand side of Eq. (4), the bulk nematic-isotropic phase transition from $S=0$ to $S_b=\sqrt{6}/4\approx 0.612$ occurs at $\tau_b=\tau_{NI}(h=0)=1/8$. Here I rederive the temperature that the first-order bulk nematic-paranematic phase transition in the presence of a magnetic field occurs [10]. Figure 1 illustrates the bulk free energy in the presence of a magnetic field. The absolute minimum of the free energy corresponds to the stable phase. The phase transition occurs when the two values of the free energy in minimums will be equal. If S_{m1} and S_{m3} are the minimums in the bulk free energy, the condition of phase transition is $f_b(S_{m1})=f_b(S_{m3})$ (see Fig. 1). The nematic-paranematic phase transition in the presence of a magnetic field occurs from S_{m1} to S_{m3} at $\tau_{NI}(h)$. On the basis of such arguments, the bulk phase transition temperature versus the reduced magnetic field is calculated and it is drawn in Fig. 2. It has a linear behavior. The equation of this line is $h=0.612\tau-0.0765$. It is noted that the bulk nematic-isotropic phase transition in the absence of a magnetic field from $S=0$ to $S_b(h=0)\approx 0.612$ occurs at $\tau_b=\tau_{NI}(h=0)=\frac{1}{8}$, thus the slope of the line in Fig. 2 is the order parameter in the bulk phase in the absence of a magnetic field. The line in Fig. 2 separates the regions of the paranematic and nematic phases. The nematic phase is stable in above the line. When crossing the line, nematic-paranematic transition occurs and so the bulk phase is in the paranematic state.

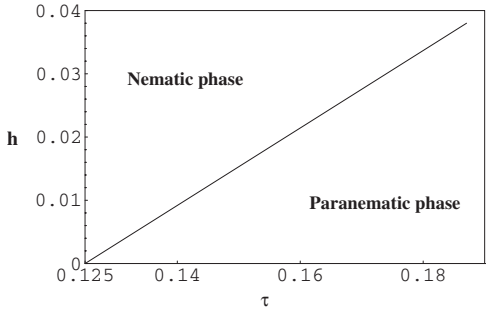

FIG. 2. Variation of the bulk nematic-paranematic temperature as a function of a reduced magnetic field. It illustrates a linear behavior between transition temperature and a magnetic field. Above and below the line, the bulk phase is nematic and paranematic, respectively. When crossing the line the bulk experiences the first-order nematic-paranematic phase transition.

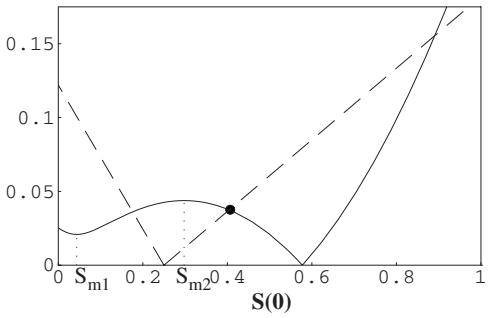

FIG. 3. Graphical solution of Eq. (13) for $\tau < \tau_{NI}$, $0 < S_0 < S_b$, and $h=0.01$. The straight lines correspond to $\gamma|S(0)-S_0|$ and the curved to $\sqrt{f_b(S(0))-f_b(S_b)}$. The dot indicates the absolute minimum of the free energy F_A.

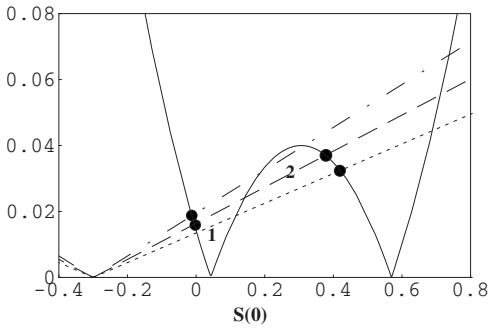

FIG. 4. Graphical solution of Eq. (13) for $\tau=\tau_{NI}$, $S_0<0$, and $h=0.01$. The straight lines correspond to $\gamma|S(0)-S_0|$ and the curved to $\sqrt{f_b(S(0))-f_b(S_b)}$. The dots indicate the absolute minimum of the free energy F_A. The free energies of the first three solutions differ by the areas 1 and 2 enclosed by the curved and one of the straight lines. With increasing γ, a value is passed where the areas 1 and 2 are equal (Maxwell construction) and where the absolute minimum $S(0)$ jumps.

III. WETTING IN THE PRESENCE OF A MAGNETIC FIELD

I will study wetting below τ_{NI} both for surface-induced prolate order ($S>0$), where the liquid-crystal molecules align preferentially along the surface normal, but also for oblate order ($S<0$), where they want to be parallel to the interface [17]. However, the second case has to be considered with caution since one expects biaxial orientational ordering as several studies for temperatures above τ_{NI} have already shown [14,29,30].

Variation of the free energy (7) in order to determine the order parameter profile $S(z)$ that minimizes F_A gives the Euler-Lagrange equation for the bulk,

$$\frac{d^2S}{d^2z} = \frac{1}{2}\frac{df_b}{dS}, \tag{9}$$

and the two boundary conditions at the interface,

$$\left.\frac{dS}{dz}\right|_{z=0} = \gamma[S(0) - S_0], \tag{10}$$

and far from it,

$$\left.\frac{dS}{dz}\right|_{z\to\infty} = 0 \quad \text{or} \quad \lim_{z\to\infty} S(z) = S_b, \tag{11}$$

where the orientational order is uniform and where it assumes the bulk value S_b, determined by minimizing the bulk free energy density f_b of Eq. (8). Integrating the Euler-Lagrange equation (9) once and determining the integration constant from boundary condition (11), gives

$$\left|\frac{dS}{dz}\right| = \sqrt{f_b(S) - f_b(S_b)}. \tag{12}$$

Finally, this formula together with boundary condition (10) at the interface, determines the order parameter $S(0)$ at the interface as follows:

$$\gamma|S(0) - S_0| = \sqrt{f_b(S(0)) - f_b(S_b)}. \tag{13}$$

For $\tau \leqslant \tau_{NI}(h)$, Figs. 3 and 4 illustrate graphical representations of Eq. (13) for $0 < S_0 < S_b$ and $S_0 < 0$, respectively. The full line and dashed line relate to the right and the left side of Eq. (13), respectively. When multiple solutions for $S(0)$ occur, the correct $S(0)$ is that one which gives the absolute minimum value of the free energy. Combining Eqs. (7) and (12) and using a transformation of the integration variable from z to S under the reasonable assumption that $S(z)$ is monotonic, one ultimately arrives at

$$F_A = K \pm 2\int_{S(0)}^{S_b} [\sqrt{f_b(S) - f_b(S_b)} \mp \gamma(S - S_0)]dS, \tag{14}$$

with the constant $K=f_b(S_b)d-\gamma(S_b-S_0)^2$, where d is the sample dimensionless thickness. $f_b(S_b)d$ is the bulk free energy, when the whole sample would exhibit bulk order [3]. The upper and lower signs refer to $dS/dz \geqslant 0$ and $dS/dz \leqslant 0$, respectively. The first case occurs, e.g., for $\tau \leqslant \tau_{NI}$ when $S(z)$ approaches $S_b=S_{m3}$ starting from $S(0)<S_b$ and the second case applies to $\tau \geqslant \tau_{NI}$ when $S(z)>0$ decays monotonically to $S_b=S_{m1}$ [see curve (3) in Fig. 5]. For the situation illustrated in Fig. 4, a graphical representation of F_A is possible: the free energies of the different solutions $S_i(0)$ differ

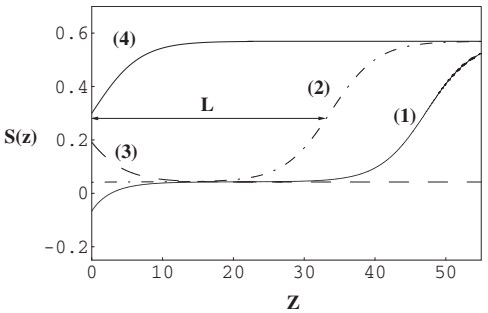

FIG. 5. Order parameter profiles $S(z)$ as a function of distance from a substrate close to or at the nematic-isotropic phase transition temperature for different parameters: (1) $S_0=-0.2$, $\gamma=0.3$, $h=0.01$, $\tau=0.141\,32\,99$; (2) $S_0=0.04$, $\gamma=0.2$, $h=0.01$, $\tau=\tau_{NI}(h)=0.141\,33$; (3) $S_0=0.3$, $\gamma=0.3$, $h=0.0099$, $\tau=0.141\,33<\tau_{NI}(h)$; (4) $S_0=0.1$, $\gamma=0.2$, $h=0.01$, $\tau=\tau_{NI}(h)=0.141\,33$. The thickness L of the wetting layer is defined by the inflection point farthest away from the interface at $z=0$. The coordinate z is given in units of ξ.

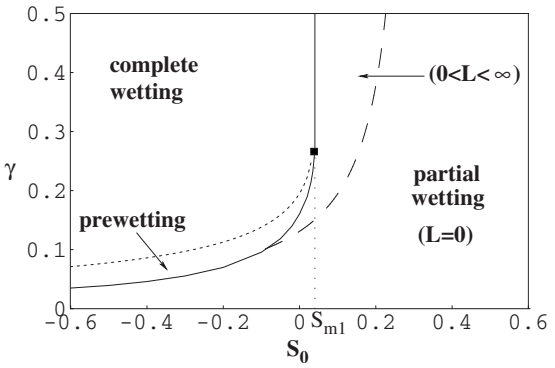

FIG. 6. Wetting diagram for isotropic wetting when $\tau_{NI}(h)$ is approached from below, in the parameter space of the surface potential: reduced anchoring strength γ versus rescaled preferred order parameter S_0 for $h=0.01$. The filled square indicates a tricritical point at (0.043,0.2985) for the wetting transitions. The position of the tricritical point depends on the magnetic field.

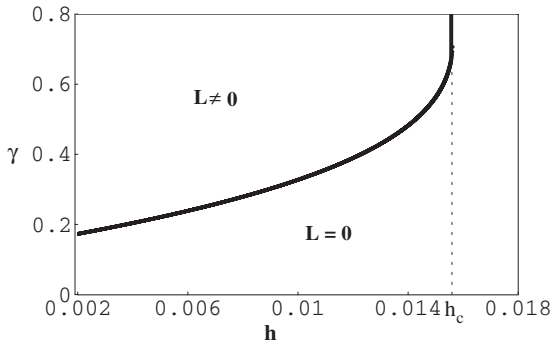

FIG. 7. Behavior of the wetting layer. The vertical full line indicates the second transition.

by the areas 1 and 2 enclosed by the curved and one of the straight lines. The dots indicate the absolute minimum of the free energy F_A. A transition between different solutions $S_i(0)$ occurs if areas 1 and 2 are both the same, which is called Maxwell construction. In this case a prewetting transition between different wetting profiles occurs.

Once $S(0)$ is obtained, the $S(z)$ profile is calculated through the integral of Eq. (12) for a monotonic order profile as follows:

$$z = \pm \int_{S(0)}^{S(z)} \frac{dS}{\sqrt{f_b(S) - f_b(S_b)}}. \tag{15}$$

Figure 5 presents a profile of order parameter just before and after the nematic-isotropic transition temperature. Curve (1) in Fig. 5 presents a complete wetting of the interface with a paranematic phase can occur for $\tau \to \tau_{NI}(h)$ at $h=h_{NI}$, $S_0 \to S_{m1}$, and $\gamma > \gamma_c$ (γ_c is defined in the next section). Curve (4) in Fig. 5 illustrates a nematic wetting for $\tau \to \tau_{NI}(h)$ at $h=h_{NI}$ close to the substrate. To quantify the thickness of wetting layers, one notes that every extremum S_m in the bulk free energy f_b gives rise to an inflection point in the profile $S(z)$ as stated by the Euler-Lagrange equation (9). The thickness L of a wetting layer by the distance of the inflection point from the interface is defined as follows:

$$L = \pm \int_{S(0)}^{S_m} \frac{dS}{\sqrt{f_b(S) - f_b(S_b)}}. \tag{16}$$

If two inflection points exist, the one with the largest distance is chosen. Whenever $f_b(S)$ approaches $f_b(S_b)$, a singularity occurs in the definition (16) and L diverges as I will demonstrate for $\tau \leqslant \tau_{NI}$ as a function of the magnetic field in the next section.

IV. PARANEMATIC WETTING

Consider a bulk phase is in the nematic phase. I will discuss how the paranematic phase wets the interface in the presence of the magnetic field when the the nematic-isotropic (paranematic) phase transition is approached from below. Figure 6 illustrates the relevant wetting phase diagram in the parameter space of the surface potential. The full line separates the regions of the complete wetting and partial wetting. In the second case, the nematic order parameter close to the interface is reduced relative to the bulk value. The curved part of the full line is determined by the Maxwell construction, when areas 1 and 2 in Fig. 4 are equal. The dotted line is the projection of a critical line on the S_0, γ plane at $\tau_{NI}(h)$. The confined region between the dotted and full line defines the prewetting surface. When crossing this region with decreasing temperature, the order parameter profile jumps from the thick film to the thin film. The curved and vertical part of the wetting line (full line) meet in a tricritical point at $(S_{m1}, \gamma_c = \frac{\partial}{\partial S}\sqrt{f_b(S) - f_b(S_b)})$, which is indicated by the filled square. The position of this point just depends on the magnetic field strength [e.g., (0.043,0.2985) for $h=0.01$]. My colleagues and I illustrated that the position of this point is (0,0.354) in the absence of a magnetic field [17]. The dashed line in the partial-wetting regime divides a region where the wetting layer, following definition (16), has zero thickness L, from a region with $L \neq 0$. In the case of $L=0$, the maximum S_{m2} in the free energy is smaller than $S(0)$ (see Fig. 3) so that the profile $S(z)$ does not have an inflection point; see curve (4) in Fig. 5 as an example. In the region $(0 < L < \infty)$, the profile has one inflection point [see, e.g., curve (2) in Fig. 5]. When at $\tau = \tau_{NI}(h)$ the vertical part of the wetting line in Fig. 6 is approached, L starts to diverge [see, e.g., curve (1) in Fig. 5]. This leads to a singularity in Eq. (16) for L since $f_b(0) = f_b(S_b) = 0$ at $\tau = \tau_{NI}(h)$. Concentrating on this singularity, one finds a logarithmic divergence for L which is a function of reduced magnetic strength.

$$L \cong \int_{S(0)}^{S_{m2}} \frac{dS}{\sqrt{\tau_{NI} S^2 - hS}} \cong \frac{-1}{\sqrt{\tau_{NI}}} \ln[-h + 2\tau_{NI} S(0)]. \tag{17}$$

So on approaching the vertical part of the wetting line in the wetting phase diagram (Fig. 6), a second-order transition occurs.

Figure 7 represents a wetting phase diagram for paranematic wetting below τ_{NI} in terms of the surface anchoring strength γ, and the reduced magnetic field h. The curved line separates a region where the wetting layer has $L=0$ from a region with $L \neq 0$. The curved and vertical part of the wetting

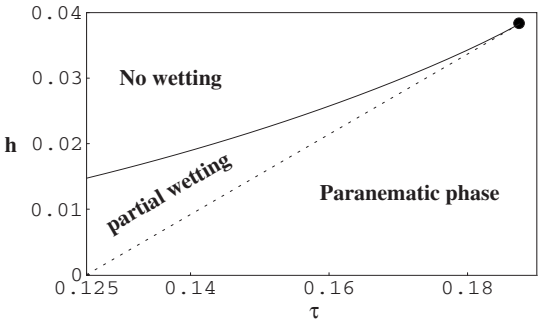

FIG. 8. Calculated magnetic field as a function of temperature. The dashed line corresponds to the first-order bulk transition h_{NI} and the full line corresponds to Eq. (18). Above the full line L is zero and the bulk phase will be pure nematic, but the region between the two lines, the behavior of wetting depends on γ. The two lines meet each other at $(\frac{3}{16}, \frac{\sqrt{6}}{64})$ which is indicated by the filled circle. Above this point, variation of the order parameter is gradual.

line meet each other at h_c. It is determined when the two extremums S_{m1} and S_{m2} in the bulk free energy (see Fig. 1) merge to one point. For arbitrary temperatures, it leads to

$$h_c = \frac{-3\sqrt{3} + 3\sqrt{3-16\tau} + 8(3\sqrt{3} - 2\sqrt{3-16\tau})}{48\sqrt{2}}. \quad (18)$$

Figure 8 presents h_c and h_{NI} as a full and dashed line, respectively. Above the full line the length of disorder layer L is zero and the bulk phase is pure nematic, but the region between the two lines, the behavior of wetting depends on γ and S_0. The dashed and full lines meet each other in a tricritical point at $(\tau_c^* = \frac{3}{16}, h_c^* = \frac{\sqrt{6}}{64})$, which is indicated by a filled circle. At (τ_c^*, h_c^*) the three extremums of the bulk free energy merge to one point; after that the bulk free energy just has one extremum and the second-order phase transition occurs. However, when crossing the dashed line a first-order nematic-paranematic phase transition occurs while above the tricritical point the evolution of the order parameter is gradual [31]. The experimental study shows that a wetting transition changes from first order to continuous with increasing surface anchoring [27]. In the weak surface anchoring, Boamfa *et al.* find that the surface transition has a sharp first order. It is a combination of first-order and continuous in the medium anchoring energy and it is continuous for strong anchoring [27].

V. DISCUSSION AND CONCLUSIONS

The influence of an external magnetic field on the prewetting transition and on the wetting behavior of a nematic liquid crystal with positive magnetic anisotropy has been studied using a phenomenological Landau–de Gennes model. Wetting has been studied in the presence of a magnetic field not only for surface-induced prolate order ($S>0$), where the liquid-crystal molecules align preferentially along the surface normal, but also for oblate order ($S<0$), where they want to be parallel to the interface. I have assumed that the order parameter is uniaxial everywhere. The thermodynamic phase diagram has been calculated. Solving the free energy equation numerically, it has been found that the magnetic field could increase first-order transition temperature as a linear behavior with the zero field bulk order parameter slope which terminates at the tricritical point. After that the variation of the order parameter is gradual. Although some parts of my results were observed experimentally [27], my results are valid for weak homeotropic anchoring. I only considered a uniaxial nematic liquid crystal with positive magnetic anisotropy. On the basis of experimental observation, the phase is uniaxial in the presence of a magnetic field [27]. In the case that magnetic anisotropy is negative, the magnetic field creates the second axis and the phase becomes biaxial, which is not considered in this paper.

[1] B. Jérôme, Rep. Prog. Phys. **54**, 391 (1991).
[2] G. P. Crawford, R. J. Ondris-Crawford, J. W. Doane, and S. Žumer, Phys. Rev. E **53**, 3647 (1996).
[3] P. Sheng, Phys. Rev. A **26**, 1610 (1982).
[4] S. Kralj, S. Žumer, and D. W. Allender, Phys. Rev. A **43**, 2943 (1991).
[5] J. I. Fukuda, H. Stark, and H. Yokoyama, Phys. Rev. E **69**, 021714 (2004).
[6] M. I. Kaganov and A. N. Omelyanchuk, Sov. Phys. JETP **34**, 895 (1972).
[7] K. Binder and P. C. Hohenberg, Phys. Rev. B **6**, 3461 (1972).
[8] A. Poniewierski and T. J. Sluckin, Mol. Cryst. Liq. Cryst. **111**, 373 (1984).
[9] P. G. de Gennes and J. Prost, *The Physics of Liquid Crystals*, 2nd ed. (Oxford Science Publications, Oxford, 1993).
[10] J. Hanus, Phys. Rev. **178**, 420 (1969).
[11] P. J. Wojtowicz and P. Sheng, Phys. Lett. **48A**, 235 (1974).
[12] I. Lelidis and G. Durand, Phys. Rev. E **48**, 3822 (1993).
[13] C. Fan and M. Stephen, Phys. Rev. Lett. **25**, 500 (1970).
[14] T. J. Sluckin and A. Poniewierski, Phys. Rev. Lett. **55**, 2907 (1985).
[15] H. Stark, J. Fukuda, and H. Yokoyama, J. Phys.: Condens. Matter **16**, S1911 (2004).
[16] J.-B. Fournier and P. Galatola, Europhys. Lett. **72**, 403 (2005).
[17] E. Kadivar, Ch. Bahr, and H. Stark, Phys. Rev. E **75**, 061711 (2007).
[18] M. M. Telo da Gama, Mol. Phys. **52**, 611 (1984).
[19] J. H. Thurtell, M. M. Telo da Gama, and K. E. Gubbins, Mol. Phys. **54**, 321 (1985).
[20] Z. Pawlowska, T. J. Sluckin, and G. F. Kventsel, Phys. Rev. A **38**, 5342 (1988).
[21] B. Tjipto-Margo, A. K. Sen, L. Mederos, and D. E. Sullivan, Mol. Phys. **67**, 601 (1989).
[22] A. M. Somoza, L. Mederos, and D. E. Sullivan, Phys. Rev. E **52**, 5017 (1995).
[23] E. M. del Rio, M. M. Telo da Gama, E. de Miguel, and L. F.

Rull, Phys. Rev. E **52**, 5028 (1995).
[24] I. Rodríquez-Ponce, J. M. Romero-Enrique, E. Velasco, L. Mederos, and L. F. Rull, Phys. Rev. Lett. **82**, 2697 (1999).
[25] E. F. Gramsbergen, L. Longa, and W. H. de Jeu, Comput. Phys. Rep. **4**, 135 (1986).
[26] P. G. de Gennes, Mol. Cryst. Liq. Cryst. **12**, 193 (1971).
[27] M. I. Boamfa, M. W. Kim, J. C. Maan, and Th. Rasing, Nature (London) **421**, 149 (2003).
[28] M. Nobili and G. Durand, Phys. Rev. A **46**, R6174 (1992).
[29] N. Kothekar, D. W. Allender, and R. M. Hornreich, Phys. Rev. E **49**, 2150 (1994).
[30] M. Huber and H. Stark, Europhys. Lett. **69**, 135 (2005).
[31] S. Kralj and V. Popa-Nita, Eur. Phys. J. E **14**, 115 (2004).